Modelling and Control of a novel SOFC-IC Engine Hybrid System

Alexandros Plianos * **Anita R. Chaudhari** **
Richard K. Stobart ***

* *Department of Aeronautical and Automotive Engineering, Loughborough University, Loughborough, UK (e-mail:a.plianos@lboro.ac.uk)*
** *Department of Aeronautical and Automotive Engineering, Loughborough University, Loughborough, UK (e-mail:a.r.chaudhari@lboro.ac.uk)*
*** *Department of Aeronautical and Automotive Engineering, Loughborough University, Loughborough, UK (e-mail:r.k.stobart@lboro.ac.uk)*

Abstract: A novel configuration of a Solid Oxide Fuel Cell-Internal Combustion (SOFC-IC) engine is presented and a nonlinear dynamic model that captures the transient phenomena of this system is developed. A variable geometry turbocharger and a throttle present at the air inlet is used to regulate the interacting flows in the combined system. A controller is developed to regulate the output to demand specific setpoints which correspond to the required power output of the hybrid vehicle. The controller is derived by means of identified linear models. It consists of a feedback term, an integral term and a feedforward term. An observer is used for the estimation of the system states. The nonlinear system is assessed under closed-loop control with simulations.

1. INTRODUCTION

Fuel cells have emerged as a viable technology in automotive propulsion technologies to reduce harmful emissions. The Polymer Electrolyte Membrane (PEM) fuel cell is generally regarded as the preferred choice in automotive applications. However PEM has several disadvantages. The anode is sensitive to carbon monoxide (CO) and should be fed only with pure hydrogen. This requires a hydrogen tank fitted on the vehicle and the appropriate hydrogen distribution infrastructure. Alternatively, if a reformer is used, the CO in the outlet of the reformer has to be eliminated. In addition, PEMs require sophisticated water management and humidification of the incoming flows to hydrate the membrane for good function of the fuel cell. In contrast, Solid Oxide Fuel Cell (SOFC) can operate with CO in the anode. The high operating temperatures of the SOFC and the increased availability of vapor water in the anode, allow internal reforming and thus a reformer is not essential (Rajashekara et al. [2006]). Their restricted use in automotive propulsion is mainly due to long start-up times and inability to respond quickly in transient power demand. These considerations are not very limiting if the SOFC is used as an auxiliary power unit (APU) (see Botti et al. [2005]) or in a hybrid configuration.

Currently, the SOFC has been combined with a battery to extent the range of a series hybrid vehicle or combined with a battery driving an electric machine and an internal combustion driven system operating as a parallel hybrid vehicle.

This paper is concerned with a novel SOFC-IC engine architecture where the exhaust flows from the anode and the cathode fed to the engine. Effects of hydrogen induction in a diesel fuelled engine have been studied by Mathur et al. [1992] and Mathur et al. [1993]. The studies show improvements in thermal efficiency of the engine with increasing amount of hydrogen in the engine. However, the thermal efficiency rapidly decreases when the amount of hydrogen in the cylinder increased above 20%. With the use of nitrogen as a diluent, the amount of hydrogen added, without deteriorating the thermal efficiency can be increased. It also assists in reducing knocking in the engine caused by introduction of hydrogen. The dilution of the air charge with nitrogen, vapour water and carbon dioxide (if internal reforming is used) can reduce the combustion temperature and thus reduce the formation of NO_x. The reduction of the combustion temperature is caused by reducing the oxygen concentration, dilution effects and the higher heat capacity of water and CO_2 as reported in Ladommatos et al. [1996a], Ladommatos et al. [1996b], Ladommatos et al. [1997a] and Ladommatos et al. [1997b]. On this basis, the system proposed below utilizes the exhausts from the fuel cell to provide hydrogen and nitrogen into the diesel-fuelled engine.

The modeling and control approach of the proposed hybrid configuration has been inspired from work reported in the literature regarding stand alone fuel cell systems and has been extended to the current hybrid system. Some publications relevant to this work include:Pukrushpan et al. [2002], Pukrushpan et al. [2004a], Qi et al. [2006], and Kandepu et al. [2005].

The rest of the paper is structured as follows. In section 2, a brief description of the system is given. Then, a nonlinear model of the hybrid airpath is presented in section 3. Section 4 is devoted to the control law design . Finally, simulation results are presented in section 5.

2. SYSTEM DESCRIPTION

The simulated hybrid configuration is based on a Caterpillar 3126B 6-cylinder , 205kW medium duty engine and a 60kW SOFC stack consisting of 960 cells. The stack architecture, which has 40 bundles in series, each bundle consisting of 8-in-series by 3-in-parallel has been designed in such a way so that the stack polarization is within an efficient operating region.

The schematic diagram of the hybrid SOFC-IC engine air system under investigation, is depicted in figure 1. The fresh air is first compressed and then split into two paths. A portion of the flow is directed to the intake manifold through a throttle, with the rest of the flow fed into the cell cathode. The compressor is driven by a variable nozzle turbine which converts the exhaust gas energy into shaft work. On turbines with variable geometry, the inlet vanes are guided to vary the area of a nozzle which controls the flow through the turbine. The throttle is used to partially restrict the direct flow into the inlet manifold, increasing the pressure at the compressor outlet which in effect increases the flow through the fuel cell cathode.

The manipulation of the turbine vanes position in coordination with the throttle position allows regulation of the inlet flows. The amount of air in the cathode determines the amount of hydrogen that can be utilized. An excess of air is needed in the cathode at all times to avoid oxygen starvation which can damage the fuel cell. Similarly, the amount of fuel burnt in the cylinders is limited by the quantity of the supplied fresh air charge. The air-to-fuel (AFR) has to be beyond a certain lower limit to avoid the generation of visible smoke.

A common approach in the compression of the fresh air in fuel cells is the use of an electrically driven compressor consuming a substantial portion of the fuel cell power output. In this proposed configuration, the net power output of the fuel cell is significantly increased by using the energy of the exhaust gases, instead. An adverse effect is that there is some energy loss associated with throttling the incoming flow. Moreover and in order to sustain the same compressor flow of un-throttled operation, the compressor power requirement is increased due to the increased pressure upstream the throttle.

It should be noted that this configuration can be used at high engine loads only. At low load conditions in which the engine is disabled, an auxiliary electrically driven compressor can be used to increase cathode pressure.

The air path control problem is complicated due to the nonlinear nature of the turbocharger, strong interaction between the fuel cell and VGT flow paths through the dynamics of the compressor outlet volume and the common shaft between the compressor and the turbine. In the next section, we propose a dynamic model of the airpath system. The Mean Value Engine Model (MVEM) has been validated against experimental data. The turbocharger

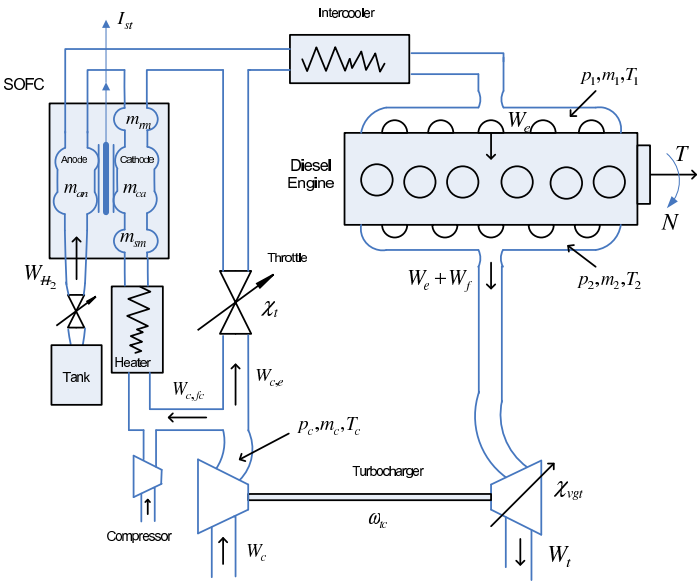

Fig. 1. Hybrid Air system Configuration

maps have been scaled so that provide a better match with the studied configuration. The parameters of the fuel cell model used, have been taken from Xue et al. [2005] and they have been scaled according to the fuel cell volume.

3. MODELING OF THE SOFC-IC ENGINE HYBRID SYSTEM

3.1 Turbocharger Model

The dynamics of the turbocharger rotational speed ω is governed by

$$\dot{\omega}_{tc} = \frac{1}{J_{tc}\omega_{tc}}(\eta_m P_t - P_c) \tag{1}$$

where η_m is the mechanical efficiency of the turbocharger, and P_t, P_c are the turbine and compressor power, respectively. The turbine and compressor powers are parameterized from maps provided from the manufacturer. Compressor power is regressed in turbospeed, compressor flow and compressor pressure ratio. Turbine power is regressed in turbospeed, turbine flow, turbine pressure ratio,and vanes position. A detailed description of the turbocharger parameterizations used can be found in Plianos and Stobart [2008].

3.2 Nonlinear Fuel Cell System Model

A nonlinear dynamic model which captures the flow dynamics and power generation of the SOFC is developed. The fuel cell flow characterization is based on the emptying and filling principle which has been widely used to model fuel cell flow dynamics (for example see Pukrushpan et al. [2004]). In developing the model, a uniform temperature distribution across the FC is assumed. This can be achieved by regulation of a heater at the inlet of the FC.

The FC model consists of the following six states: m_{O_2} mass of oxygen in the cathode (kg), m_{N_2} mass of nitrogen in the cathode (kg), m_{H_2} mass of hydrogen in the anode

(kg), m_{H_2O} mass of water in the anode (kg), m_{sm} mass of air in the cathode's supply manifold (kg), m_{rm} mass of air in the cathode's return manifold (kg).

The conservation of mass implies the following equations for the mass balance of oxygen and nitrogen inside the cathode volume.

$$\begin{cases} \dot{m}_{O_2} = W_{O_2,in} - W_{O_2,out} + W_{O_2,used} \\ \dot{m}_{N_2} = W_{N_2,in} - W_{N_2,out} \end{cases} \tag{2}$$

where $W_{O_2,in}$, $W_{O_2,out}, W_{O_2,used}$ are the oxygen flow in, out and crossing the membrane, respectively. $W_{N_2,in}$, $W_{N_2,out}$ are the corresponding nitrogen flows in and out the cathode volume.

The corresponding mass balance of hydrogen and water in the anode is

$$\begin{cases} \dot{m}_{H_2} = W_{H_2,in} - W_{H_2,out} + W_{H_2,used} \\ \dot{m}_{H_2O} = W_{H_2O,in} - W_{H_2O,out} + W_{H_2O,gen} \end{cases} \tag{3}$$

where $W_{H_2,in}$, $W_{H_2,out}, W_{H_2,used}$ are the hydrogen flow in, out and consumed, respectively. $W_{H_2O,in}$,$W_{H_2O,out}$,$W_{H_2O,gen}$ are the corresponding water vapor flows in, out and generated in the anode volume, respectively.

Since the air is heated to a constant value after the compressor stage, the rate of mass in the supply manifold of the cathode is only necessary to describe the filling and emptying dynamics. Thus

$$\dot{m}_{sm} = W_{c,fc} - W_{sm,out} \tag{4}$$

The pressure differential across the supply manifold outlet is low allowing the flow $W_{c_{sm,out}}$ to be modelled as

$$W_{sm,out} = k_{sm,out}(p_{sm} - p_{ca}) \tag{5}$$

where $k_{sm,out}$ is the supply manifold outlet coefficient. p_{sm}, p_{ca} are the pressure in the supply manifold and cathode, respectively. The inlet flow of the supply manifold is described by the orifice equation:

$$W_{c,fc} = k_{sm,in}\frac{p_{sm}}{\sqrt{RT_c}}\Psi(\frac{p_{sm}}{p_c}) \tag{6}$$

where $k_{sm,in}$ is the supply manifold inlet coefficient and p_c, T_c are the pressure and temperature in the compressor outlet volume. The pressure dependant term Ψ is given by

$$\Psi(\frac{p_{sm}}{p_c}) = \begin{cases} \gamma^{0.5}(\frac{2}{\gamma+1})^{((\gamma+1)/2(\gamma-1))} \\ if \frac{p_{sm}}{p_c} \leq (\frac{2}{\gamma+1})^{(\gamma/(\gamma-1))} \\ \sqrt{\frac{2\gamma}{\gamma-1}((\frac{p_{sm}}{p_c})^{2/\gamma} - (\frac{p_{sm}}{p_c})^{(\gamma+1)/\gamma})} \\ if \frac{p_{sm}}{p_c} \geq (\frac{2}{\gamma+1})^{(\gamma/(\gamma-1))} \end{cases} \tag{7}$$

The return manifold can be modeled in the same way as the supply manifold using equations (4,5,6, 7) replacing $k_{sm,out}$, $k_{sm,in}$, p_{sm},p_{ca}, p_c, T_c with $k_{rm,out}$, $k_{rm,in}$, p_{rm}, p_1, p_{ca}, T_{sm}. Isothermal conditions in the cathode and the anode allow the partial pressure of the species in the cathode and anode to be calculated from the ideal gas low.

$$p_i = \frac{1}{V_i} m_i R T_{ts} \tag{8}$$

The stack voltage output V_{fc} of the fuel cell is expressed as

$$V_{fc} = E - (R_a + R_c + R_\omega)I_{st} \tag{9}$$

where E is the Nernst potential (V), I_{st} is the stack current (A), R_ω is the stack ohmic resistance (Ω). R_a, R_c are the equivalent resistances of the anode and the cathode, respectively, which are expressed as

$$R_a = \left[\frac{4F}{RT} k_A \frac{p_{H_2}}{p_{an}}^{0.25} exp(-\frac{U_a}{RT}) \right]^{-1} \tag{10}$$

$$R_c = \left[\frac{4F}{RT} k_c \frac{p_{O_2}}{p_{ca}}^{0.25} exp(-\frac{U_c}{RT}) \right]^{-1} \tag{11}$$

where F is the Faraday constant (Coulombs), T_{st} is the stack temperature. k_a, k_c are the pre-exponential factor of the anode and cathode, respectively. U_a, U_c is the activation energy of the anode and cathode, respectively. The Nernst potential E is given by

$$E = -\frac{\Delta G^o}{2F} + \frac{RT_{st}}{2F} ln(\frac{p_{H_2} p_{O_2}^{0.5}}{pH_2O}) \tag{12}$$

where ΔG^o is the Gibbs free energy at atmospheric pressure.

The rates of oxygen reacted, hydrogen reacted and water generated linearly depend on fuel cell current according to the electrochemical equations:

$$\begin{cases} W_{O_2,used} = M_{O_2}\frac{nI_{st}}{4F} \\ W_{H_2,used} = M_{H_2}\frac{nI_{st}}{2F} \\ W_{H_2O,gen} = M_{H_2O}\frac{nI_{st}}{2F} \end{cases} \tag{13}$$

where n is the number of cells in the stack, F is the Faraday number and M_{O_2}, M_{H_2} ,and M_{H_2O} are the molar mass of oxygen, hydrogen and vapour water, respectively. The total pressures in the cathode and anode are the sum of the species contained, thus

$$\begin{cases} p_{ca} = p_{O_2} + p_{N_2} \\ p_{an} = p_{H_2} + p_{H_2O} \end{cases} \tag{14}$$

3.3 Diesel Engine Airpath Model

The engine model consists of the following ten states: m_1 mass of gas in the intake (kg), m_2 mass of gas in the exhaust manifold (kg), m_c mass of gas in the compressor outlet volume (kg), p_1 intake manifold pressure (kPa), p_2 exhaust manifold pressure (kPa), p_c pressure in the compressor outlet volume (kPa), F_{N_2} fraction of nitrogen in the intake manifold, F_{H_2O} fraction of water in the intake manifold, F_{H_2} fraction of hydrogen in the intake manifold, F_2 fraction of exhaust gases in the exhaust manifold.

Applying the principle of mass conservation in the intake plenum, exhaust plenum, and the volume of the compressor outlet, the mass balance state equations are given

$$\begin{cases} \dot{m}_1 = W_{c_e} + W_{rm_{out}} - W_e \\ \dot{m}_2 = W_e - W_t + W_f \\ \dot{m}_c = W_c - W_{c,e} - W_{c,fc} \end{cases} \tag{15}$$

Applying the principle of energy conservation in the intake plenum, exhaust plenum, and the volume of the compressor outlet, the pressure state equations are given

$$\begin{cases} \dot{p}_1 = \dfrac{\gamma R}{V_1}(W_{rm,out}T_{st} + W_{c,e}T_c - W_eT_1) \\ \dot{p}_2 = \dfrac{\gamma R}{V_2}[(W_e + W_f)T_e - W_tT_1] \\ \dot{p}_c = \dfrac{\gamma R}{V_c}(W_cT_{cc} - W_{c,e}T_c - W_{c,fc}T_c) \end{cases} \tag{16}$$

The parameterizations of flow into the cylinders, engine temperature can be found in Plianos and Stobart [2008]. The rate of change of the fraction of nitrogen, water, hydrogen in the intake plenum and exhaust gases in the exhaust are given.

$$\begin{cases} \dot{F}_{N_2} = \dfrac{W_{c_e}(.79 - F_{N_2}) + W_{rm_{out}}(\frac{m_{N_2}}{m_{N_2}+m_{O_2}} - F_{N_2})}{m_1} \\ \dot{F}_{H_2O} = \dfrac{W_{an,out}(\frac{m_{H_2O}}{m_{H_2O}+m_{H2}}) - (W_{an,out} - W_{c,e})F_{H_2O}}{m1} \\ \dot{F}_{H_2} = \dfrac{W_{an,out}(\frac{m_{H_2}}{m_{H_2O}+m_{H2}}) - (W_{an,out} - W_{c,e})F_{H_2}}{m1} \\ \dot{F}_2 = \dfrac{1}{m_2}\left(W_e[15.6(1 - F_1)/(AFR + 1) + F_1] - W_eF_2\right) \end{cases} \tag{17}$$

The flow through the throttle is described by the orifice equation:

$$W_{c,e} = k_c(\chi_c)\frac{p_c}{\sqrt{RT_c}}\Psi(\frac{p_1}{p_c}) \tag{18}$$

where k_c is the throttle flow coefficient and p_c is the pressure in the compressor outlet volume. The pressure dependant term Ψ is given in equation (7).

4. AIRPATH CONTROL DESIGN

4.1 Control Objective

The fuel cell related performance objective is to regulate the oxygen excess ratio λ_{O_2}, fuel cell power output and hydrogen utilization μ_f to a desirable value. The oxygen excess ratio is defined as

$$\lambda_{O_2} = \frac{W_{sm,out}}{W_{O_2,used}} \tag{19}$$

and the utilization factor as

$$\mu_f = \frac{W_{H_2,used}}{W_{an}} \tag{20}$$

Thus, the performance variable vector relevant to the fuel cell operation is defined as:

$$z_{fc} = [\, P_{fc} \;\; \lambda_{O_2} \;\; \mu_f \,]^T \tag{21}$$

The value opted for λ_{O_2} is 1.8 which is sufficient to avoid oxygen starvation. A higher value is not used in order to reduce excessive throttling, reduce the compressor power consumed and reduce the heating and cooling efforts. The utilization factor is maintained at .85, a value which allows an efficient operation of the cell but also provides a fraction of hydrogen to enter the cylinders. The third variable, fuel cell power setpoint is combined with the equivalent engine power to meet load requirements.

Similarly, the control objective for the engine is to regulate Oxygen-to-Fuel ratio (OFR), fraction of nitrogen and water in the intake manifold, F_t and power output P_{ic}. The OFR is defined as

$$OFR = \frac{(1 - F_{N_2} - F_{H_2O} - F_{H_2})W_e}{W_f + F_{H_2}W_e} \tag{22}$$

and F_t is given by

$$F_t = F_{N_2} + F_{H_2O} \tag{23}$$

OFR is restricted to values above 4.2 to avoid formation of visible smoke and F_t should be as high as possible. The engine performance vector is then given as

$$z_{fc} = [\, P_e \;\; OFR \;\; F_t \,]^T \tag{24}$$

Since all performance variables are difficult to measure in a production vehicle, other variables which can be easier to measure, are used for regulation. The output vector selected herein consists of intake manifold pressure and cathode flow. Thus

$$y = [\, p_1 \;\; W_{c,fc} \,]^T \tag{25}$$

The selected output correlates with the performance variables in steady state conditions. The stack current and hydrogen inlet flow are functions of the fuel cell power setpoint, i.e. $I_{st} = f^d_{fc}(P^d_{fc})$, $W_{H_2} = f^d_{fc}(P^d_{fc})$. Similarly, the engine speed and fuel rate are functions of the engine power setpoint, i.e. $N = f^d_{ic}(P^d_{ic})$, $W_{W_f} = f^d_{ic}(P^d_{ic})$.

4.2 Controller Design

The controller development is based on a pair of low order linear models identified from the sixteenth order nonlinear model around the setpoints. The model was excited with PRBS signals with a frequency range consistent with the intended system operational frequency. Rather than using a direct linearization of the nonlinear model, identification was used to emulate the controller design process of the real process. The most consistent identification results were obtained using models of fourth order and the Prediction Error Method (PEM) algorithm. The structure of the identified models is

$$\begin{aligned} x(k+1) &= Ax(k) + B_u u(k) + B_w w(k) \\ y(k+1) &= Cx(t) \end{aligned} \tag{26}$$

with $x(k) \in R^4$ the state of the model, $u(k) = [\chi_t, \chi_{vgt}]^T \in R^2$ the control input and $w(k) = [I_{st}, W_f, N]^T \in R^3$ the external input. The states of the identified model do not have a physical interpretation, however they are a linear combination of the physical states of the system. The identifier selection of states is determined so that the input-output response characteristics are captured and the identified system is both controllable and observable.

The proposed controller consist of state feedback with integral action and feedforward compensation. It has the following form:

$$u = -K(\hat{x} - x^d) + K_I \int (\hat{x} - x^d)dt + u^d \tag{27}$$

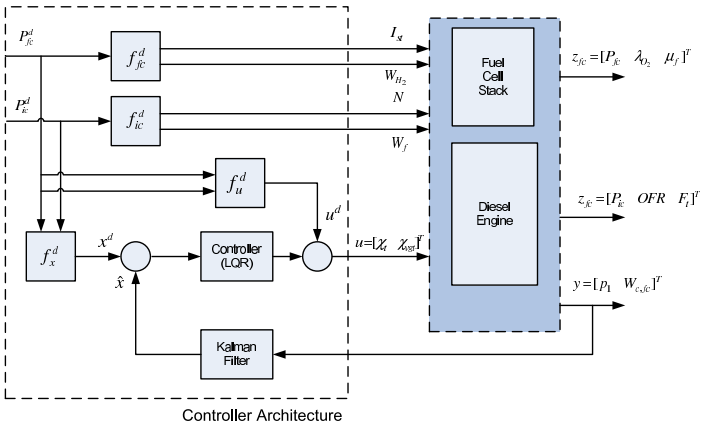

Fig. 2. Simulation Model

An estimated state $\hat{x}$ is used in the control law (27). It is estimated using a simple linear state-observer. The parameters of the controller are gain-scheduled as a function of the external input w. The feedforward u^d and state setpoints x^d are scheduled in systems power setpoints, thus $u^d = f_u^d(P_{fc}^d, P_{ic}^d)$, $x^d = f_x^d(P_{fc}^d, P_{ic}^d)$.

5. SIMULATION RESULTS

In order to validate the control design based on the linear identified models, we apply the state feedback control law to the nonlinear engine model. The closed-loop configuration of the nonlinear simulation engine model is shown in fig. 2. The model includes the dynamics of the actuators which are both modeled as first order lags. The parameters of the VGT actuator are identified from test cell experimental data in frequency domain, whilst the throttle actuator transfer function has a time constant of a typical automotive throttle.

A sequence of simultaneous power demand of the fuel cell and the engine, step changes from setpoint 1 to setpoint 2 and vice versa is used as an excitation signal of the closed-loop system. Setpoint values for the performance, output variables and input positions are listed in table 1.

Figure 3 shows the response of the system's output. During the step change in power demand, the first output, intake manifold pressure exhibits a small overshoot and responds significantly slower that the cathode's air flow. This difference in outputs timescales signifies the control authority of each actuator to vary each of the output variables. The VGT vane position has a greater authority on the inlet pressure, whilst the throttle position is more effective in manipulating cathode flow. Thus, the lag between VGT vanes position and compressor power output acts to slow the build-up of inlet pressure. The throttle position can rapidly change the pressure ratio across the throttle itself and thus the cathode flow dynamics are inherently fast. The inlet pressure exhibits non minimum phase behavior due to the interaction of the two different timescales.

The response of the engine performance variables and fuel cell performance variables are shown if fig. 4 and fig. 5, respectively. Moreover, the input trajectories are depicted in fig. 6. Note that the power outputs of the

Table 1. Operating Points

Variable	Setpoint 1	Setpoint 2
y_1 (bar)	1.97	2.53
y_2 (kg/s)	0.044	0.052
λ_{O_2} (-)	1.8	1.8
P_{fc} (kW)	25	39
λ_{O_2} (-)	0.086	0.15
μ_f (-)	0.85	0.85
P_{ic} (kW)	90	46
OFR (-)	5.3	6.5
F_t (-)	0.86	0.87
χ_t (-)	0.7	0.45
χ_{vgt} (-)	0.4	0.1

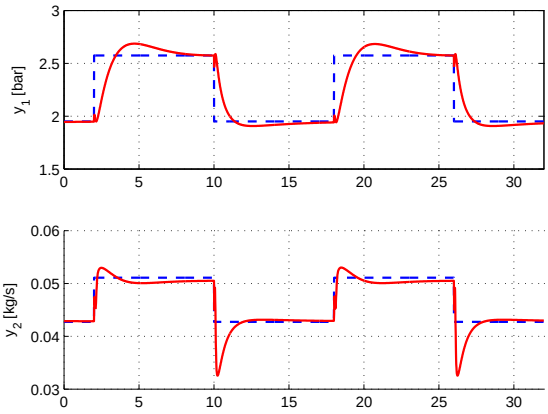

Fig. 3. Reference trajectories (dashed) versus Output responses (solid)

engine and fuel cell shown in figures 4, 5 have been derived from static relationships as the simulated model does not include the dynamics of the engine crankshaft, electric motor and drivetrain. Good regulation of the outputs results in achieving the desired response of the performance variables. Regarding engine performance, the OFR is maintained at high enough levels to avoid the generation of visible smoke at all times. Moreover, the concentration of dilution species in the intake manifold is maintained above 0.85, while the concentration of non combustible species for normal air is around 0.79. In the fuel cell part, the oxygen excess variable is kept above one at all times even though it reaches the proximity of one when cathode's flow is low. In addition, the feed-forward term, f_{fc}^d regulates the utilization factor to the desirable value of 0.85.

6. CONCLUSIONS

A new hybrid configuration of a SOFC-IC engine has been proposed to reduce the parasitic power losses of the fuel cell and provide a means of dilution in the diesel combustion. Mathematical models for the components relevant to the hybrid airpath have been developed and flow interactions have been captured. A gain-scheduled controller is developed based on low order identified models. The controller achieves good transient performance which provides some robustness through the explicit integral term.

REFERENCES

J.J. Botti, M.J. Grieve, J.A. MacBain. Electric Vehicle Range Extension using an SOFC APU. *SAE World*

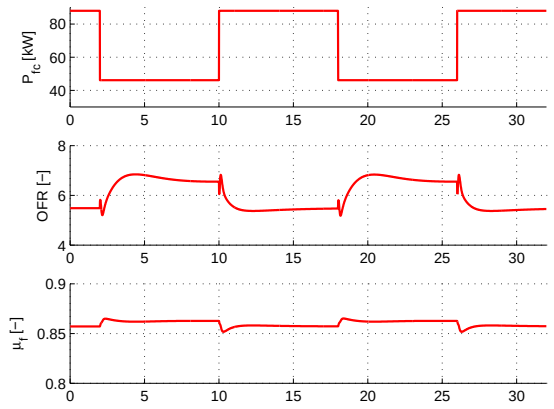

Fig. 4. Response of the engine performance variables

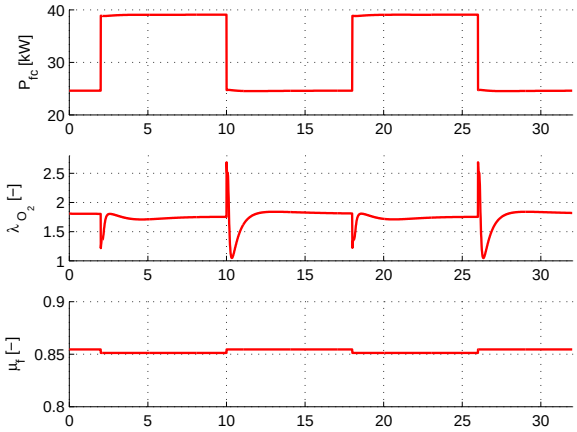

Fig. 5. Response of the fuel cell performance variables

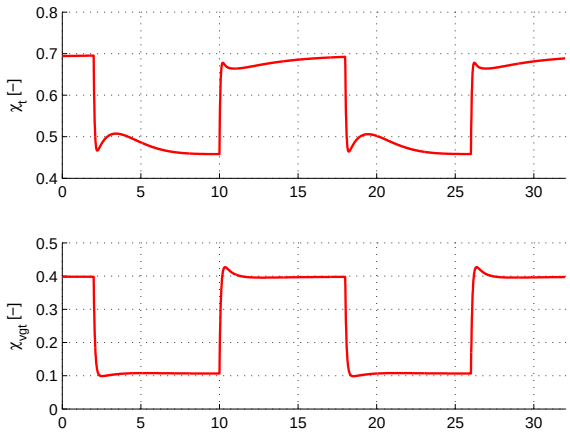

Fig. 6. Response of the actuators

Congress, Detroit, USA, Paper No. 2005-01-1171, April 2005.

A. Chaudhari,R. Stobart. Investigation of Optimum Operating Range for a Solid Oxide Fuel Cell-IC Engine Hybrid System. *IEEE Conference on Electric and Hybrid Vehicles, ICEHV '06*, pages 1–6, 2006.

A. Chaudhari, A. Plianos, R. Stobart. Modelling and Control Design of SOFC-IC Engine Hybrid System. *2008 SAE World Congress, Detroit, USA*,Paper No. 2008-01-0082, April 2008.

R. Kandepu, L. Imsland,B.A.Foss, C. Stiller, B. Thorud, O. Bolland. Control-relevant SOFC Modeling and Model Evaluation. *Proceedings of ECOS 2005*, pages: 1139–1145, Trondhein, Norway, June 20-22, 2005.

N. Ladommatos,S.M. Abdelhalim, H. Zhao, Z. Hu. The Dilution, Chemical, and Thermal Effects of Exhaust Gas Recirculation on Diesel Engine Emissions Part 1: Effect of Reducing Inlet Charge Oxygen. SAE Paper No. 961165.

N. Ladommatos, S.M. Abdelhalim, H. Zhao, Z. Hu. The Dilution, Chemical, and Thermal Effects of Exhaust Gas Recirculation on Diesel Engine Emissions Part 2: Effects of Carbon Dioxide. SAE Paper No. 961167.

N. Ladommatos, S.M. Abdelhalim, H. Zhao, Z. Hu. The Dilution, Chemical, and Thermal Effects of Exhaust Gas Recirculation on Diesel Engine Emissions Part 3: Effects of Water Vapour. SAE Paper No. 971659.

N. Ladommatos, S.M. Abdelhalim, H. Zhao, Z. Hu. The Dilution, Chemical, and Thermal Effects of Exhaust Gas Recirculation on Diesel Engine Emissions Part 4: Effects of Carbon Dioxide and Water Vapour. SAE Paper No. 971659.

H.B. Mathur, L.M. Das, T.N. Patro. Hydrogen fuel utilization in CI engine powered end utility systems. *Int J. Hydrogen Energy*, 17:369–374, 1992.

H.B. Mathur, L.M. Das, T.N. Patro. Hydrogen-Fuelled Diesel Engine: Performance Improvement Through Charge Dilution Techniques. *Int J. Hydrogen Energy*, 18:421–431, 1993.

A. Plianos, R.K.Stobart. Modeling and Control of Diesel Engines Equipped with a Two-Stage Turbo-System. SAE Paper No. 2008-01-1018.

J.T. Pukrushpan, A.G. Stefanopoulou, H. Peng. Modeling and Control of Fuel Cell PEM Stack Systems. *Proceedings of the American Control Conference*, pages: 3117–3122, Anchorage, AK,2002.

J.T. Pukrushpan, A.G. Stefanopoulou, H. Peng. Control of fuel cell power systems : principles, modeling, analysis, and feedback design. Springer, New York, 2004.

J.T. Pukrushpan, A.G. Stefanopoulou, H. Peng. Controlling Fuel Cell Breathing. *in IEEE Control Systems Magazine*, 24(2):30–46, 2004.

Y. Qi,B. Huang, J. Luo. Nonlinear State Space Modeling and Simulation of A SOFC Fuel Cell. *Proceedings of the 2006 American Control Conference*, pages: 2535–2538, Minnesota, USA, June 14-16, 2006.

K. Rajashekara, J.A. Macbain, M.J Grieve. Evaluation of SOFC Hybrid Systems for Automotive Propulsion Applications. *Proceedings of the IEEE Industry Applications Conference*, 3:1593–1593, 2006.

X. Xue, J. Tang, N. Sammes,Y. Du. Dynamic modeling of single tubular SOFC combining heat/mass transfer and electrochemical reaction effects *Journal of Power Sources*, 142:211–222, 2005.